

## High-Energy Neutrinos from Photomeson Processes in Blazars

Armen Atoyan<sup>1</sup> and Charles D. Dermer<sup>2</sup>

<sup>1</sup>*CRM, Universite de Montreal, Montreal H3C 3J7, Canada*

<sup>2</sup>*Code 7653, Naval Research Laboratory, Washington, D.C. 20375-5352*

(Received 30 June 2001; published 7 November 2001)

An important radiation field for photomeson neutrino production in blazars is shown to be the radiation field external to the jet. Assuming that protons are accelerated with the same power as electrons and injected with a  $-2$  number spectrum, we predict that  $\text{km}^2$  neutrino telescopes will detect  $\geq 1$  neutrinos per year from flat spectrum radio quasars such as 3C 279. The escaping high-energy neutron and photon beams transport inner jet energy far from the black-hole engine, and could power synchrotron x-ray jets and FR II hot spots and lobes.

DOI: 10.1103/PhysRevLett.87.221102

PACS numbers: 98.54.Cm, 96.40.Tv, 98.62.Nx, 98.70.Rz

EGRET observations of  $\approx 100$  MeV–5 GeV emission from over 60 flat spectrum radio quasars (FSRQs) and BL Lac objects established that blazars are, with gamma-ray bursts, among the most powerful accelerators of relativistic particles in nature [1]. The standard blazar model consists of a supermassive black hole ejecting twin jets of relativistic plasma, one of which is pointed towards us. Bright, highly variable nonthermal radiation from blazars means that regions of intense photon and nonthermal particle energy densities, both of which are needed for efficient photopion production [2,3], are found in these sources. Blazars therefore represent a potential source of energetic  $\pi^\pm$ -decay neutrinos to be detected by operating and planned high-energy neutrino telescopes [4]. Previous treatments have considered internal synchrotron photons and the direct disk radiation field [5] as targets for high-energy proton interactions in jets, and neutrino production in the cores of AGN (active galactic nuclei) [6]. Here we show that photons from external quasi-isotropic radiation fields, which have earlier been proposed as target photons to be Compton-scattered by nonthermal electrons to  $\gamma$ -ray energies [7], also provide the most important photon source for photomeson production of  $\geq 30$  TeV neutrinos in FSRQs. The inclusion of this effect increases neutrino production rates by more than an order of magnitude. Moreover, the neutrinos are formed at energies  $\geq 3 \times 10^{13}$  eV rather than at  $\geq 10^{17}$  eV [8], which improves prospects for detection.

Strong optical emission lines from the illumination of broad-line region (BLR) clouds reveal bright accretion disk and scattered disk radiation [7] in the inner regions of FSRQs. BL Lac objects are blazars with weak emission lines, so the dominant soft photon field there is thought to be the internal synchrotron emission. In our analysis of photomeson production in FSRQs, we assume that the quasi-isotropic scattered external radiation field dominates the direct accretion disk field. The photomeson neutrino spectrum can be calculated once the mean magnetic field and comoving spectral energy density are determined. The measured variability time scale  $t_{\text{var}}$  and synchrotron ( $L_s$ ) and Compton ( $L_c$ ) luminosities determined from the

spectral energy distribution of the bright, well-studied blazar 3C 279 [9] implies physical parameters of its jet emission region. Its redshift  $z = 0.538$ , which implies a luminosity distance  $d_L \approx 1.05 \times 10^{28}$  cm for a standard cosmology. A crucial unknown is the Doppler factor  $\delta = [\Gamma(1 - \beta_\Gamma \cos\theta)]^{-1}$ , where  $\Gamma$  is the bulk Lorentz factor of the relativistic plasma blob, and  $\theta$  is the angle between the jet and observer directions.

The comoving synchrotron photon energy density is given by  $u'_s \approx L_s / (2\pi r_b^2 c \delta^4)$ , where  $r_b$  is the comoving radius of the blob, here assumed spherical, and primes denote comoving quantities. The spectral energy density  $u'_s(\epsilon') \equiv m_e c^2 \epsilon' n'_s(\epsilon')$  (units of  $\text{ergs s}^{-1} \epsilon'^{-1}$ ) of photons with dimensionless comoving energy  $\epsilon' = h\nu'/m_e c^2$  is found through

$$\epsilon' u'_s(\epsilon') \approx \frac{2d_L^2 f_s(\epsilon)}{r_b^2 c \delta^4} \approx \frac{2d_L^2 (1+z)^2 f_s(\epsilon)}{c^3 t_{\text{var}}^2 \delta^6}, \quad (1)$$

in terms of the  $\nu F_\nu$  flux  $f_s(\epsilon)$  of the synchrotron component. Here  $\epsilon = \delta \epsilon' / (1+z)$ , and we relate  $t_{\text{var}}$  and  $r_b$  through the expression  $r_b \approx ct_{\text{var}} \delta / (1+z)$ .

For calculations of  $n'_s(\epsilon')$  from 3C 279, we approximate the flux density  $F(\epsilon) \propto \epsilon^{-\alpha}$  observed during the flare of 1996 [10] in the form of a continuous broken power-law function, with indices  $\alpha_1 \approx 0.5$ ,  $\alpha_2 \approx 1.45$ , and  $\alpha_3 \approx 0.6$  at frequencies  $\nu_0 < \nu \leq \nu_1 = \nu_{\text{pk}}$ , with  $\nu_{\text{pk}} \approx 10^{13} \nu_{13}$  Hz,  $\nu_1 \leq \nu \leq \nu_2 = 10^{16}$  Hz, and  $\nu \geq \nu_2$ , respectively. The  $\nu F_\nu$  synchrotron radiation flux  $f_s(\epsilon)$  reaches a maximum value  $f_s(\epsilon_{\text{pk}}) \approx 1.7 \times 10^{-10} \text{ erg cm}^{-2} \text{ s}^{-1}$  at  $\nu = \nu_{\text{pk}}$  or  $\epsilon = \epsilon_{\text{pk}}$ . The flaring and three-week average flux of the Compton  $\gamma$ -ray component peaks at  $\sim 500$  MeV and is  $\sim 20$  and  $\sim 5$ – $10$  times larger than  $f_s(\epsilon_{\text{pk}})$  at the corresponding times [10]. Using  $t_{\text{var}}(d) \approx 1$  (in days) for 3C 279 as observed by EGRET [10] one finds from Eq. (1) with  $\delta_{10} \equiv \delta/10$  that

$$u'_s \approx \epsilon'_{\text{pk}} u'_s(\epsilon'_{\text{pk}}) \approx 0.4 [t_{\text{var}}(d)]^{-2} \delta_{10}^{-6} \text{ erg cm}^{-3}. \quad (2)$$

If the  $\gamma$  rays from FSRQs are due to Compton scattering of external photons, then  $L_{\text{EC}}/L_s \approx u'_{\text{ext}}/u_B$  [7], where  $L_{\text{EC}} = L_c - L_{\text{SSC}}$  is the measured power from Compton-scattered external photon fields, and  $L_{\text{SSC}}$  is the

synchrotron-self-Compton (SSC) power. Consequently  $u'_{\text{ext}} \cong u_B(L_{\text{EC}}/L_s) = au'_s = aL_s/(2\pi r_b^2 c \delta^4)$ , where  $a \equiv L_{\text{EC}}/L_{\text{SSC}}$ . The energy of the external photons in the comoving frame is  $\epsilon'_{\text{ext}} \cong \delta \epsilon_{\text{ext}}$ . Models taking into account SSC and external Compton (EC) components show that a complete spectral fit requires synchrotron, SSC and EC components [11], with  $a \sim 0.1$ – $1$  for BL Lac objects and  $a \sim 1$ – $10$  for FSRQs. During the 1996 flare of 3C 279,  $a \approx 10$ , so that the energy density of external soft photons in the comoving blob frame is  $\sim 10\times$  greater than the synchrotron energy density.

Lower limits to  $\delta$  are defined by the condition that the emitting region be transparent to  $\gamma\gamma$  pair-production

$$B(\text{Gauss}) \cong 130 \frac{d_{28}^{4/7} f_{-10}^{2/7} [(1 + k_{pe}) \ln(\nu_0/\nu_1)]^{2/7} (1+z)^{5/7}}{\eta^{2/7} [t_{\text{var}}(d)]^{6/7} \delta^{13/7} \nu_{13}^{1/7}}, \quad (3)$$

where  $\nu_0/\nu_1 \cong 10^3$  and  $f_{-10} \equiv f_s(\epsilon_{\text{pk}})/(10^{-10} \text{ erg cm}^{-2} \text{ s}^{-1}) = 1.7$  for 3C 279.

An alternative estimate of  $B$  can be derived from the observed synchrotron and Compton powers [13]. Neglecting Klein-Nishina effects on Compton scattering, the ratio of the Compton and synchrotron powers  $L_C/L_s \cong u'_{\text{ph}}/u_B$ , so that  $u_B = (L_s/L_C)u'_s(1 + u'_{\text{ext}}/u'_s) = (L_s/L_C)u'_s(1 + a)$ . Using Eq. (1) in this expression for  $B$  gives

$$B(\text{Gauss}) \cong \frac{2(1+z)}{\delta^3 t_{\text{var}}} \frac{L_s \sqrt{1+a}}{c^{3/2} L_C^{1/2}}. \quad (4)$$

The observed flux of synchrotron radiation from 3C 279 with  $\alpha = 0.5$  at  $\nu \leq 10^{13}$  Hz implies that  $B(\text{G}) \cong 7\eta^{-2/7} [t_{\text{var}}(d)]^{-6/7} \delta_{10}^{-13/7}$  from equipartition arguments. The estimate of  $B$  from Eq. (4) gives  $B(\text{G}) \cong 4t_{\text{var}}^{-1}(d)\delta_{10}^{-3}$ , using  $L_s = 3 \times 10^{47} \text{ ergs s}^{-1}$ ,  $L_C/L_s \cong 10$ , and  $a \cong 10$ . The external radiation energy density in the comoving frame, using  $B$  derived from Eq. (3), is  $u'_{\text{ext}} \cong 1.5(L_{\text{EC}}/L_s)\eta^{-4/7} [t_{\text{var}}(d)]^{-12/7} \delta_{10}^{-26/7} \text{ erg cm}^{-3}$ . Note the weaker dependence of  $u'_{\text{ext}}$  on  $\delta$  compared to  $u'_s$ . For the calculations we take  $\eta = 1$  and  $L_{\text{EC}}/L_s = 10$ .

Energy losses of relativistic protons (and neutrons) are calculated on the basis of standard expressions (e.g., Ref. [14]) for the cooling time of relativistic protons due to photopion production in  $p\gamma$  collisions. If the ambient photons have spectral density  $n'_{\text{ph}}(\epsilon')$ , then

$$t_{p\gamma}^{-1}(\gamma_p) = \int_{\epsilon_{\text{th}}/2\gamma_p}^{\infty} d\epsilon' \frac{cn'_{\text{ph}}(\epsilon')}{2\gamma_p^2 \epsilon'^2} \times \int_{\epsilon_{\text{th}}}^{2\epsilon'\gamma_p} d\epsilon_r \sigma(\epsilon_r) K_{p\gamma}(\epsilon_r) \epsilon_r,$$

where  $\gamma_p$  is the proton Lorentz factor,  $\epsilon_r$  is the photon energy in the proton rest frame,  $\sigma(\epsilon_r)$  is the photopion production cross section,  $\epsilon_{\text{th}} \approx 150$  MeV is the threshold energy for the parent photon in the proton rest frame, and  $K_{p\gamma}(\epsilon_r)$  is the inelasticity of the interaction. The latter increases from  $K_1 \approx 0.2$  at energies not very far above the threshold to  $K_2 \sim 0.5$ – $0.6$  at larger values of  $\epsilon_r$  where multipion production dominates [14,15].

attenuation inside the blob [12], which requires that  $\tau_{\gamma\gamma}(\epsilon') \cong 2\sigma_T n'_s (2/\epsilon') r_b / (3\epsilon') < 1$ . The measured  $>10^{16}$  Hz flux during the 1996 flare then implies that  $\delta \geq 5[E_{\text{ph}}(\text{GeV})^{0.12}/t_{\text{var}}(d)]^{0.19}$ , where  $E_{\text{ph}}(\text{GeV})$  is the photon energy in GeV.

The magnetic field  $B$  in the blob can be determined by introducing the equipartition parameter  $\eta = u'_{el}(1 + k_{pe})/u_B$  for the ratio of relativistic electron to magnetic energy densities in the jet, with the factor  $k_{pe}$  correcting for the presence of nonthermal hadrons. We assume  $k_{pe} = 1$  in the estimate of  $B$ . The measured synchrotron flux density  $F_\nu \propto \nu^{-\alpha}$  with  $\alpha \approx 0.5$  at  $\nu \leq 10^{13}$  Hz gives the equipartition magnetic field

A detailed recent study of this photohadronic process is given by Ref. [15]. To simplify calculations, we approximate  $\sigma(\epsilon_r)$  as a sum of two step functions  $\sigma_1(\epsilon_r)$  and  $\sigma_2(\epsilon_r)$  for the total single-pion ( $p + \gamma \rightarrow p + \pi^0$  or  $n + \pi^+$ ) and multipion channels, respectively, with  $\sigma_1 = 380 \mu\text{b}$  for  $200 \leq \epsilon_r \leq 500$  MeV and  $\sigma_1 = 0$  outside this region, whereas  $\sigma_2 = 120 \mu\text{b}$  at  $\epsilon_r \geq 500$  MeV. The inelasticity is approximated as  $K_{p\gamma} = K_1$  and  $K_{p\gamma} = K_2$  below and above 500 MeV. Our calculations give good agreement with more detailed treatments [15–17] of both the time scale  $t_{p\gamma}$  and the mean inelasticity  $K_{p\gamma}$  for photomeson interactions.

The spectra of secondary  $\pi^{0,\pm}$ -decay particles ( $\nu, \gamma, e$ ) are calculated in the  $\delta$ -function approximation, assuming that the probabilities for producing pions of different charges ( $\pi^0, \pi^+, \text{ and } \pi^-$ ) are equal for the multipion interaction channel. To correctly apply the  $\delta$ -function approximation, one has to properly take into account the different inelasticities of the multipion and single-pion production channels (see Ref. [15] for comparison).

We assume that the spectrum of the external UV radiation field arises from a Shakura and Sunyaev [17] optically thick accretion disk model that is scattered by BLR clouds. This disk model has flux density  $F(\epsilon) \propto \epsilon^{1/3} \exp(-\epsilon/\epsilon_{\text{max}})$ , where the maximum photon energy  $\epsilon_{\text{max}}$  is determined by the innermost radius of the blackbody disk and properties of the central engine. We take  $m_e c^2 \epsilon_{\text{max}} = 35$  eV [18].

Figure 1 shows observer-frame energy loss time scales of protons due to photopion production in a jet of 3C 279. For comparison, we show also the photopion time scales if only the interactions with the synchrotron radiation were taken into account for the cases  $\delta = 7$  and  $10$ . Figure 2 shows the energy distributions of relativistic protons  $N_p(E)$  in the jet plasma blobs calculated assuming power-law injection of relativistic protons with number index  $\alpha_p = 2$  on observed time scales  $\Delta t = 3$  weeks. In calculations of  $N_p$  we take into account the photohadron interaction energy losses, as well as the escape losses of

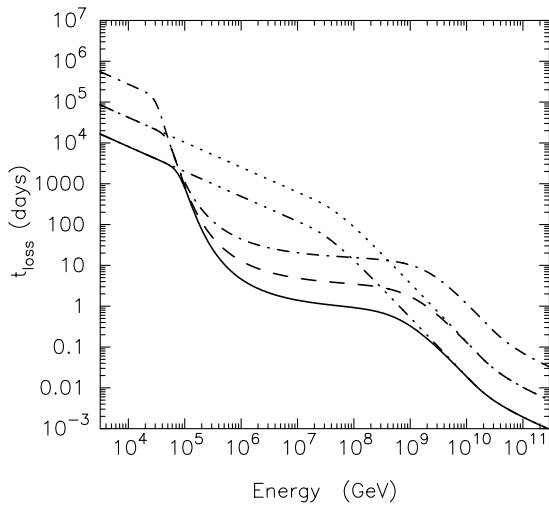


FIG. 1. Photomeson interaction energy loss time scale of protons, calculated for spectral fluxes observed from 3C 279 (see text) and  $t_{\text{var}} = 1$  d, assuming three different Doppler factors for the jet:  $\delta = 7$  (solid curve),  $\delta = 10$  (dashed curve), and  $\delta = 15$  (dot-dashed curve). The dotted and triple-dot-dashed curves are calculated for  $\delta = 7$  and  $\delta = 10$ , respectively, when  $p\gamma$  interactions with the synchrotron radiation field alone are considered.

the protons in the Bohm diffusion limit, which ensures also that the gyroradii of the highest energy ions do not exceed  $r_b$  [19].

Importantly, we also take into account proton losses through the  $p\gamma \rightarrow nX$  channel. The neutrons may then escape the blob either before they decay or collide again with photons inside the blob. To demonstrate the significance of this channel, in Fig. 2 by the full dotted curve we show the proton distribution calculated for the case of  $\delta = 7$ , but neglecting the effect of escaping neutrons.

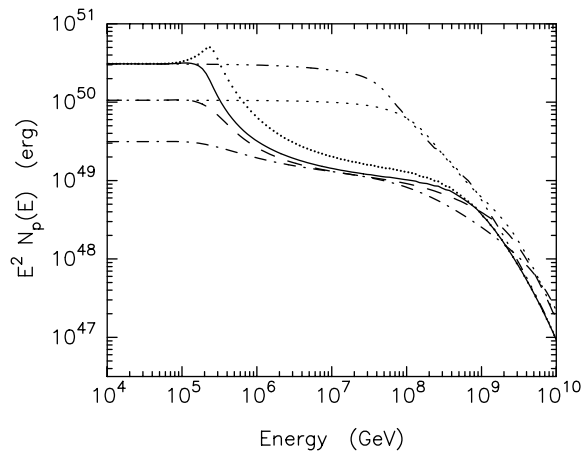


FIG. 2. The energy distribution of relativistic protons, calculated for the same jet Lorentz factors  $\delta = 7, 10,$  and  $15$  and assumptions for the external and internal radiation fields as made in Fig. 1, assuming a power-law injection of relativistic protons with number index  $\alpha_p = 2$  during  $\Delta t = 3$  weeks with a power  $L_p = 2 \times 10^{48} \delta^{-4} \text{ ergs s}^{-1}$ . The full dots show the proton distribution calculated without the effect of neutrons escaping the blob.

Comparison with the solid curve indicates that  $\approx 50\%$  of the  $E \geq 10^{14}$  eV proton energy is carried by relativistic neutrons from the blob, forming a highly collimated neutron beam with opening angle  $\theta_b \sim 1/\Gamma$  and a total power  $L_n^{(\text{beam})} \sim 0.25L_p \sim 5 \times 10^{47} \delta^{-4} \text{ erg s}^{-1}$ .

Figure 3 shows the expected differential fluences of neutrinos produced by protons in Fig. 2, integrated over the three week flaring period. Note that the mean neutrino energy fluxes at  $E \geq 100$  TeV are at the level  $E F_\nu(E) \approx E^2 \Phi_\nu / \Delta t \lesssim 2 \times 10^{-11} \text{ erg cm}^{-2} \text{ s}^{-1}$ . Given very similar emissivities in overall secondary  $\nu$  and  $(\gamma + e)$  production (e.g., Ref. [15]), the *unabsorbed* fluxes of multi-TeV  $\gamma$  rays would therefore be at the same level, which makes only  $\leq 2\%$  of the  $\gamma$ -ray energy flux detected by EGRET. A pair-photon cascade in the blob would increase this fraction to the level of  $\leq 10\%$  contribution of the cascade radiation to the detected  $\gamma$ -ray flux, reprocessing most of the initial  $\gamma$ -ray energy into  $\gamma$  radiation with  $E \lesssim 10$  GeV. A small fraction of the energy will appear as synchrotron radiation in the x-ray to GeV  $\gamma$ -ray band. Because the cascade synchrotron power is emitted with a very hard spectrum over a wide energy range, it will not overproduce also the observed x-ray flux of 3C 279.

For the fluences in Fig. 3, the total number  $N_\nu$  of neutrinos that could be detected by a  $1 \text{ km}^2$  detector, using neutrino detection efficiencies given by Ref. [4], is 0.45, 0.27, and 0.12 for the cases of  $\delta = 7, 10,$  and  $15$ , respectively. These numbers are, however, much less if the external field is neglected, namely  $N_\nu \approx 0.055$  ( $\delta = 7$ ) and  $0.014$  ( $\delta = 10$ ) for the fluences in Fig. 3. This would not leave a realistic prospect for the detection of at least 2–3 neutrinos, which is required for a positive detection of a source. BL Lac objects, which have weak BLRs and, therefore, a weak scattered external radiation field, should consequently be much weaker neutrino sources.

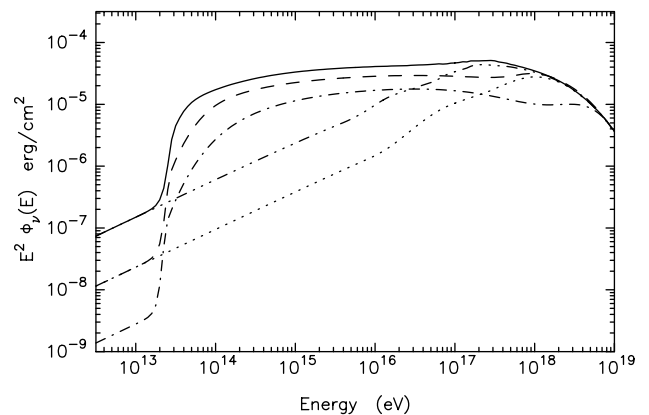


FIG. 3. The fluences of neutrinos expected due to photomeson interactions of protons shown in Fig. 2 with the external (UV) and internal (synchrotron) photons in the jet of 3C 279 for Doppler factors  $\delta = 7$  (solid curve),  $\delta = 10$  (dashed curve), and  $\delta = 15$  (dot-dashed curve). The dotted and triple-dot-dashed curves show the neutrino fluences if the external photon field in the jet is neglected.

For a 10% flaring duty factor, and considering the additional neutrino production during the quiescent phase, we expect that IceCube or other  $\text{km}^2$  arrays may detect several neutrinos per year from 3C 279-type blazar jets with  $\delta \approx 5-15$ . Allowing an overall power of protons larger than that for primary electrons improves the prospects for neutrino detection. A softer nonthermal proton spectrum would, however, reduce the neutrino emissivity.

Acceleration of protons only to  $E_p \approx 10^{14}$  eV is required for efficient neutrino production through photomeson interactions, as can be seen from Fig. 1. Thus we predict that a  $\text{km}^2$  array will detect high-energy neutrinos from FSRQs without requiring acceleration of protons to ultrahigh ( $\geq 10^{19}$  eV) energies. The maximum cosmic-ray energies from blazars are found to be  $E_{\text{CR,max}} \approx 8 \times 10^{17} Z \Gamma^2 B(G) t_{\text{var}}(d)/(1+z)$  eV [19], with maximum neutrino energies a factor  $\sim 20$  lower. Given additionally the intense photomeson interactions encountered by a proton at this optimistic limit in the jet environment (see Fig. 1), it is unlikely that the inner jets of blazars are significant sources of ultrahigh energy cosmic rays. The neutrino production from FSRQs is therefore unaffected by the cosmic ray bound of Ref. [20] (though note the more general upper limit derived in Ref. [3]).

About half of the photomeson interactions in the plasma jet will produce neutrons. Neutrons with co-moving Lorentz factors  $\gamma'_n \approx 10^3 \delta_{10} t_{\text{var}}(d)$  will escape the blob in a collimated beam, and continue to interact efficiently with the external UV radiation field up to  $\sim 0.1-1$  pc scales, initiating pair-photon cascades far away from, but in the same direction with, the inner jet due to secondary  $\gamma$  rays and electrons. FSRQ jets will thus form intense neutron and photon beams that transport energy far from the central engine of the AGN [21]. Cosmic-ray neutrons with energies of  $10^{17} E_{17}$  eV will decay at distances  $\lesssim E_{17}$  kpc from the jet core. The deposition of the energy of the beamed hadrons and multi-TeV  $\gamma$  rays (through  $\gamma\gamma$  absorption at  $>10$  kpc scales) can reasonably be at the mean rate  $\sim 10^{43}$  erg  $\text{s}^{-1}$ , which could lead to enhanced x-ray synchrotron emission along the large-scale jet, as seen by the Chandra X-ray Observatory from sources such as Pictor A [22]. Depending on the stability of charged particle transport, nonthermal particles could be deposited at  $\geq 100$  kpc to supply power for hot spots and lobes in FR II galaxies, though *in situ* particle acceleration could also take place at these sites. The predicted weaker neutron and neutrino production in BL Lac objects and their parent FR I galaxies might account for the morphological differences of these radio galaxy types. This picture will be tested by sensitive high-energy neutrino detectors, ground-based  $\geq 50$  GeV gamma-ray detectors, and GLAST [4,23].

A. A. appreciates the support and hospitality of the NRL Gamma and Cosmic Ray Astrophysics Branch during his visit when this work was initiated. The work of C. D.

is supported by the Office of Naval Research and NASA Grant No. DPR S-13756G.

- 
- [1] R. C. Hartman *et al.*, *Astrophys. J. Suppl.* **123**, 79 (1999).
  - [2] K. Mannheim and P.L. Biermann, *Astron. Astrophys.* **253**, L21 (1992).
  - [3] K. Mannheim, R.J. Protheroe, and J.P. Rachen, *Phys. Rev. D* **63**, 023003 (2001).
  - [4] T.K. Gaisser, F. Halzen, and T. Stanev, *Phys. Rep.* **258**, 173 (1995); F. Halzen, in *High Energy Gamma Ray Astronomy*, edited by F.A. Aharonian and H.J. Völk (AIP, New York, 2001), p. 43.
  - [5] K. Mannheim, T. Stanev, and P.L. Biermann, *Astron. Astrophys.* **260**, L1 (1992); K. Mannheim, *Astron. Astrophys.* **269**, 67 (1993); W. Bednarek and R.J. Protheroe, *Mon. Not. R. Astron. Soc.* **302**, 373 (1999).
  - [6] F.W. Stecker *et al.*, *Phys. Rev. Lett.* **66**, 2697 (1991); F.W. Stecker *et al.*, *Phys. Rev. Lett.* **69**, 2738 (1992).
  - [7] M. Sikora, M.C. Begelman, and M.J. Rees, *Astrophys. J.* **421**, 153 (1994); C.D. Dermer, S.J. Sturmer, and R. Schlickeiser, *Astrophys. J. Suppl.* **109**, 103 (1997).
  - [8] A. Mücke and R.J. Protheroe, in *Proceedings of the 27th International Cosmic Ray Conference, Hamburg, Germany, 2001* (Copernicus Gesellschaft, Katlenburg-Lindau, Germany, 2001), Vol. 3, p. 1153.
  - [9] R. C. Hartman *et al.*, *Astrophys. J.* **461**, 698 (1996); E. Pian *et al.*, *Astrophys. J.* **521**, 112 (1999).
  - [10] A.E. Wehrle *et al.*, *Astrophys. J.* **497**, 178 (1998).
  - [11] M. Böttcher, *Astrophys. J.* **515**, L21 (1999); R. C. Hartman *et al.*, *Astrophys. J.* **553**, 683 (2001); R. Mukherjee *et al.*, *Astrophys. J.* **527**, 132 (1999).
  - [12] L. Maraschi, G. Ghisellini, and A. Celotti, *Astrophys. J.* **397**, L5 (1992); C.D. Dermer and N. Gehrels, *Astrophys. J.* **447**, 103 (1995); *Astrophys. J.* **456**, 412(E) (1996).
  - [13] F. Tavecchio, L. Maraschi, and G. Ghisellini, *Astrophys. J.* **509**, 608 (1998).
  - [14] V.S. Berezhinskii and S.I. Grigoreva, *Astron. Astrophys.* **199**, 1 (1988).
  - [15] A. Mücke, J.P. Rachen, R. Engel, R.J. Protheroe, and T. Stanev, *Publ. Astron. Soc. Aust.* **16**, 160 (1999).
  - [16] T. Stanev, R. Engel, A. Mücke, R.J. Protheroe, and J.P. Rachen, *Phys. Rev. D* **62**, 093005 (2000).
  - [17] N.I. Shakura and R.A. Sunyaev, *Astron. Astrophys.* **24**, 337 (1973).
  - [18] C.D. Dermer and R. Schlickeiser, *Astrophys. J.* **416**, 458 (1993).
  - [19] A.M. Hillas, *Annu. Rev. Astron. Astrophys.* **22**, 425 (1984); C.A. Norman, D.B. Melrose, and A. Achterberg, *Astrophys. J.* **454**, 60 (1995).
  - [20] See E. Waxman and J. Bahcall, *Phys. Rev. D* **59**, 023002 (1999); J. Bahcall and E. Waxman, hep-ph/9902383. Limitations of this bound are discussed by R.J. Protheroe, astro-ph/9809144.
  - [21] A.M. Atoyan, *Astron. Astrophys.* **257**, 465 (1992).
  - [22] A.S. Wilson, A.J. Young, and P.L. Shopbell, *Astrophys. J.* **547**, 740 (2001).
  - [23] For information about the Gamma ray Large Area Space Telescope, see [glast.gsfc.nasa.gov](http://glast.gsfc.nasa.gov).